Numerical and Experimental Investigation of Bolted Joints Considering the Effect of Vibration

Prathamesh Bothale[1], Prathamesh Mali [1],
Tanvi Dhurvi[1] and Sendhil Kumar S [1]*

[1]*Department of Aeronautical Engineering,*
AnnasahebDange College of Engineering and Technology, Ashta, Maharashtra, India
*erssk28@gmail.com

Abstract. Modal analysis is an essential technique for evaluating the dynamic behavior of structural components such as plates, which are commonly used in aerospace, automotive, and civil engineering applications. The presence of bolted joints introduces complexities in the dynamic response due to factors like preload, friction, and contact nonlinearity. This study focuses on investigating the modal characteristics of plates with and without bolted assemblies using both numerical and experimental methods. A finite element model (FEM) is developed to simulate the influence of joint stiffness and contact conditions on natural frequencies and mode shapes. The result from the simulation is compared with experimental data to validate the model and identify discrepancies. A comprehensive review of related literature reveals that although significant progress has been made in modeling bolted joints, challenges persist in accurately capturing joint behavior due to nonlinear interface dynamics. The outcomes of this study aim to improve the understanding of jointed plate dynamics and contribute to the development of more reliable predictive models for structural design and vibration control.

Keywords: *Bolted joints, contact mechanics, damping, finite element analysis, microslip, modal analysis, structural dynamics, preload.*

1 Introduction

1.1 Background and Motivation

Structural interfaces govern the global dynamic stability, energy dissipation capabilities, and fatigue life of complex mechanical assemblies. Among temporary fastening mechanisms, bolted joints are widely implemented in aerospace and automotive structures due to their structural efficiency, ease of maintenance, and predictable load transfer capability.

However, the introduction of a bolted interface departs significantly from rigid continuity assumptions. Clamped components exhibit complex contact kinematics under dynamic loading. The resulting structural behavior is inherently non-linear, dictated by microscopic relative displacements, pressure distributions, and frictional behavior at the mating surfaces. Characterizing this dynamic signature is critical to mitigate resonant vibrations, prevent unexpected structural fatigue, and ensure structural integrity.

1.2 Problem Statement

The primary challenge in analyzing bolted assemblies involves predicting their natural frequencies and energy dissipation rates under operating conditions. Standard engineering practices frequently rely on simplified linear approximations. These linear models fail to capture three primary structural non-linearities:

- Spatial variation in contact pressure and stiffness across clamping interfaces.

S. Uppapalli and D. Chakraborty (eds.), *Proceedings of the International Conference on Mechanics, Materials and Mechatronics (ICM³ 2026)*, Atlantis Highlights in Engineering 47,
https://doi.org/10.2991/978-94-6239-764-4_9

- Interfacial microslip, which serves as the dominant mechanism for hysteretic damping.
- The functional dependence of assembly stiffness on bolt preload magnitude and attenuation.

Neglecting these localized phenomena introduces severe discrepancies between analytical predictions and physical responses, leading to either over-engineered structures or unexpected structural failures.

1.3 Role of Interfacial Non-linearities

The dynamic response of a jointed interface is driven by non-conservative frictional forces. Three distinct mechanisms govern these physics:

Contact Non-linearity: The localized stiffness matrix is not constant; it evolves as a function of external operational loads, internal bolt preloads, and local stick-slip states.

Stick-Slip Kinematics: As structural loads increase, localized contact zones transition from relative adherence (sticking) to localized relative motion (microslip) prior to gross interfacial sliding (macroslip). This macro-micro transition generates hysteretic loops, which can be analytically quantified using distributed parameter formulations such as the Iwan model.

Preload Attenuation: Clamping forces fluctuate or decay during operation due to cyclic relaxation, material embedding, or dynamic self-loosening. These variations directly alter the contact pressure profile, driving shifts in structural natural frequencies and damping properties Figure 1 illustrates the difference between linear and nonlinear structural behaviour.

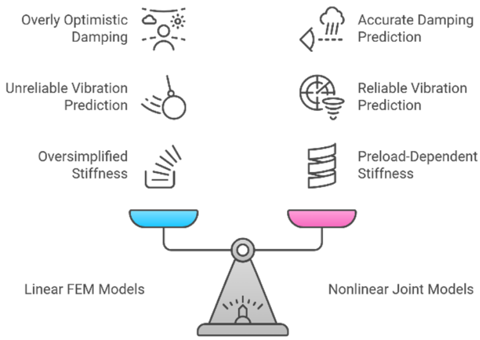

Fig. 1. Comparison between linear and non-linear behaviour.

1.4 Objectives of the Study

The primary objectives of this research are to:

- Construct a three-dimensional non-linear finite element model (NFEM) that explicitly captures localized interfacial friction and microslip mechanics.
- Characterize the functional dependence of natural frequencies on bolt preload conditions across variable joint topologies.
- Conduct harmonic vibration testing using a cost-effective MEMS data acquisition system to validate numerical frequency response profiles and track structural non-linearities.

1.5 Scope of Work

The present work is intended as a comparative investigation of the dynamic behaviour of representative bolted-joint configurations. Emphasis is placed on identifying the influence of joint geometry on modal characteristics and vibration-response trends through complementary numerical and experimental approaches. Detailed investigations involving extended operating conditions, higher excitation frequencies, and advanced correlation methodologies are beyond the scope of the current conference paper and form part of ongoing research activities.

2 Literature Review

2.1 Mechanics of Jointed Structures

Bolted joints dictate structural load-transfer paths, global stiffness distribution, and dominant failure modes in modular assemblies. Structural connections are typically categorized into friction-grip mechanical fasteners, sealed flanged joints, and geometric variants such as lap and butt configurations. Load-transfer mechanics occur primarily via shear transmission through interfacial friction or normal bearing stress against fastener hole walls. The internal stress fields induced by bolt preloads are traditionally characterized as localized pressure cones radiating from the fastener head and nut faces through the clamped components.

2.2 Non-linear Interfacial Dynamics

Under low-amplitude dynamic loads, clamped interfaces remain in a macroscopically locked state (stick region). As excitation amplitudes escalate, localized slip initiates at the boundary zones of the contact patch (microslip) before propagating into gross interfacial displacement (macroslip) under high operational stresses. This structural evolution generates a non-linear force-displacement hysteresis loop, driving amplitude-dependent damping. Mathematical formulations such as the Iwan [1], Jenkins [2], and Bouc-Wen [3] models are frequently implemented to capture these hysteretic characteristics. Variations in clamping forces induce dramatic changes in structural stiffness, leading to non-linear frequency shifts and unpredictable system behavior.

2.3 Numerical Modeling and Model Order Reduction

High-fidelity finite element methods (FEM) offer detailed insights into localized contact stresses and multi-body thread interactions. Solid-element fastener models utilizing surface-to-surface contact pairs with Coulomb friction formulations are robust options for capturing stick-slip transitions. However, the extreme computational cost of full-scale non-linear FE simulations has driven the development of Reduced-Order Models (ROMs). Traditional ROMs implement lumped parametric elements to approximate hysteretic damping [4], while modern invariant manifold techniques, such as Spectral Submanifolds (SSMs), project high-dimensional finite element equations onto low-dimensional spaces to achieve efficient computation [5].

2.4 Experimental Metrology and Parameter Identification

Experimental modal analysis (EMA) serves as the primary tool for verifying joint parameters and updating analytical formulations. Methods such as frequency-domain PolyMAX parameter estimation [6] and frequency response function (FRF) updating routines [7] are routinely deployed to align numerical models with experimental structures. Recent developments demonstrate that low-cost architectures leveraging micro-electromechanical systems (MEMS) accelerometers and open-source platforms can successfully identify fundamental frequencies, generally maintaining correlation margins within 8% of scientific instrumentation for simple configurations [8,9].

2.5 Identified Research Gaps

While progress has been made in characterizing joint dynamics, several critical challenges persist:

- Scalable ROM formulations that can concurrently handle combined multi-axial (coupled transverse and axial) operational paths remain scarce.
- Quantitative comparative studies isolating the non-linear response profiles of complex joint topologies under identical base excitations are limited.
- Explicit physics-based predictive tools tracking immediate or cycle-dependent preload loss from embedding and early-stage dynamic loosening remain underdeveloped.
- Figure 2 highlights the importance of numerical modelling in understanding structural behaviour.

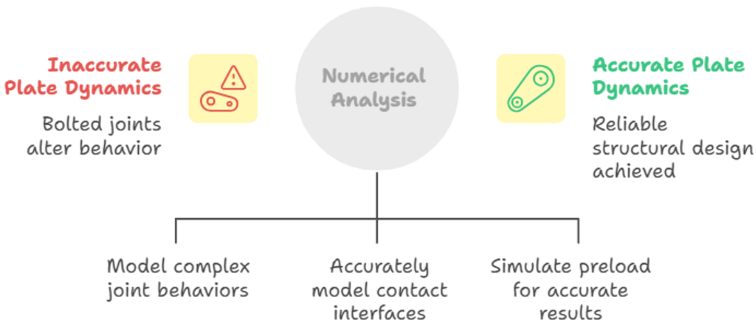

Fig. 2. Importance of numerical analysis

3 Methodology

3.1 Comprehensive Architecture

The research workflow integrates numerical modeling, structural parameterization, and experimental testing in a sequential validation pipeline. The workflow begins with geometric definition and assembly, proceeds through material property assignment and non-linear contact formulation ($\mu = 0.2$), then applies pre-stress and bolt preload (10.3 kN). The pipeline bifurcates into parallel prestrained modal FEM analysis and experimental harmonic base excitation, converging at validation and frequency spectrum analysis.

A non-linear framework is required here because conventional linear analyses cannot account for structural softening and energy dissipation caused by amplitude-dependent stick-slip transitions.

The adopted methodology combines analytical estimation, finite element modelling, and experimental vibration assessment. Each approach serves a distinct purpose within the investigation. The analytical formulation provides a baseline reference, the finite element model characterizes the modal behaviour of the jointed structures, and the experimental study evaluates vibration-response characteristics under controlled excitation conditions.

3.2 Analytical Baseline

To establish a fundamental baseline, the jointed structure is simplified analytically as an equivalent cantilever beam configuration. Utilizing standard Euler-Bernoulli beam relations, the structural properties are defined by:

$$I = \frac{bh^3}{12} \tag{1}$$

$$\omega_n = \beta_n^2 \sqrt{\frac{EI}{\rho A L^4}} \tag{2}$$

where I is the area moment of inertia, b is the beam width (40 mm), h is the plate thickness (3 mm), E is Young's modulus, ρ is the material density, A is the cross-sectional area, L is the beam length, and βn is the modal constant. This continuous beam approximation yields an idealized fundamental natural frequency of 25.541 Hz, establishing a clear baseline prior to the introduction of multi-body interface discontinuities.

3.3 Non-linear Finite Element Formulation

A three-dimensional non-linear FE model is constructed using solid elements. Fastener tension is introduced via a virtual cross-sectional pretension element technique. The contact interfaces are assigned surface-to-surface interactions governed by Coulomb friction criteria. Following the static preload step, a prestressed eigenvalue modal analysis is conducted to determine the perturbed natural frequencies and mode shapes under load-induced stress-stiffening effects:

$$[K_{effective}] = [K_{elastic}] + [K\sigma(Preload)] \tag{3}$$

Where [Kelastic] represents the linear structural stiffness matrix and [Kσ] denotes the initial stress (geometric) stiffness matrix directly generated by the fastener clamping force.

3.4 Experimental Vibration Assessment

The physical specimens are mounted in a rigid fixed-free cantilever test rig and subjected to controlled harmonic base excitation across progressive motor rotational speeds (RPM). Structural response metrics are captured via a MEMS accelerometer fixed at the free-end antinode. The raw time-domain acceleration records are transferred to a host computer and processed via a Fast Fourier Transform (FFT) routine in MATLAB to generate experimental Frequency Response Functions (FRFs).The experimental vibration assessment setup employed in the present investigation is shown in Figure 3.

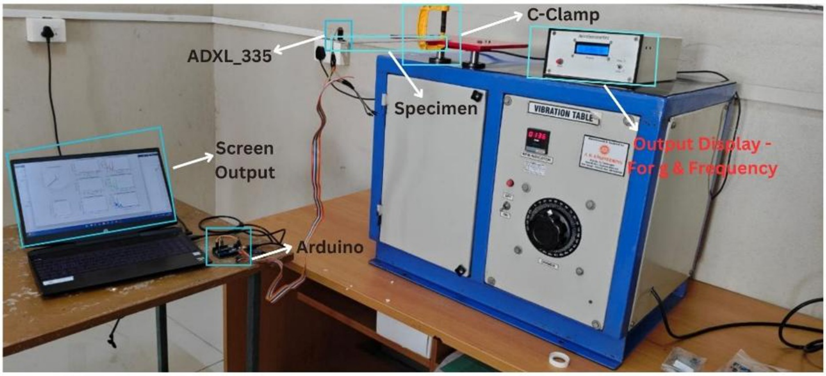

Fig. 3. Experimental setup

4 Specimen Preparations and Joint Configuration

4.1 Geometric Definitions

Three common engineering joint typologies were fabricated to evaluate the role of geometry on system dynamics:

- Substrate Geometry: Individual plates measure 200 × 40 × 3 mm.
- Fastener Specification: ISO metric M6 standard fasteners, Grade 8.8 ($\sigma y = 640$ MPa), are combined with standard steel washers to ensure uniform clamping pressure distribution.
- Hole Tolerances: Precision clearance holes are machined at Ø6.2 mm to allow realistic interfacial tolerances and localized micro-slip paths at the fastener shank boundary.

4.2 Material Properties

Clamped substrates are composed of Aluminum 6061-T6, while the fasteners are high-strength carbon steel. The constituent properties are defined in Table 1.

Table 1. Constituent material properties

Component	Material	E (GPa)	ν	ρ (kg/m³)	σy (MPa)
Substrate Plates	Al 6061-T6	68.9	0.33	2700	276
Bolt Fastener	Steel Gr. 8.8	200.0	0.30	7850	640
Flat Washer	Carbon Steel	200.0	0.30	7850	640

4.3 Contact Interface Formulation

The core non-linearity of the model relies on the surface interaction parameters. The aluminum-to-steel contact pairs are assigned an isotropic Coulomb friction coefficient ($\mu = 0.2$) based on established empirical values. Contact conditions are enforced at three critical zones:

- Plate-Plate Mating Surface: Governs primary shear transfer and interfacial sliding friction.
- Fastener Bearings: Washer-to-plate and nut-to-plate interfaces that dictate the transmission of clamping forces.
- Shank-Hole Boundary: Configured with non-penetrating boundary conditions to capture structural bearing stresses during high-amplitude transverse motion.

4.4 Preload Quantification

The target bolt pretension force is dictated by standard industrial design directives (ISO 898-1 and VDI 2230), which recommend an operational clamping force equivalent to 80% of the fastener's tensile yield limit:

$$\text{Fpreload} = 0.8 \cdot \sigma y \cdot \text{As} \tag{4}$$

Where $\sigma y = 640$ MPa and the tensile stress area for an M6 bolt is as = 20.1 mm². With the equation.4, the operational preload amounts to 10.3 kN.

4.5 Specimen Fabrication and Assembly

Aluminum 6061-T6 plates were precision-sheared, deburred, and polished to minimize surface roughness variations across test groups. Fastener clearance holes were drilled on a CNC vertical machining center to guarantee strict perpendicularity tolerances. Torque application followed the Turn-of-Nut method calibrated to settle consistently at the target pre-tension force of 10.3 kN.

5 Boundary Condition and Dynamic Loading

5.1 Numerical Constraints

The finite element boundary conditions mimic an ideal cantilever setup. The cross-sectional face of the fixed end is constrained in all six degrees of freedom ($Ux = Uy = Uz = \theta x = \theta y = \theta z = 0$). This configuration isolates compliance changes to the jointed interface.

Normal contact constraints are enforced utilizing the Penalty Method.

$$Fn = kc \cdot \delta \tag{5}$$

Where kc represents the contact stiffness factor and δ denotes the virtual penetration depth.

5.2 Experimental Implementation

Physical boundaries are enforced via a high-stiffness, high-mass steel test frame secured with a heavy-duty C-clamp fixture to replicate fixed-base boundary conditions. An ADXL-335 MEMS accelerometer is fixed to the structural free end (bending antinode) with its primary measurement axis-oriented transverse to the plate plane. Input base excitation metrics across variable motor speeds are detailed in Table 2.

5.3 Signal Acquisition and Processing

Data tracking is executed via an Arduino-based microcontroller running an onboard Analog-to-Digital Converter (ADC). Voltage transformations utilize standard scaling laws:

$$V = (ADC\_raw / 1023) \times Vcc \tag{6}$$

$$a\,[g] = (V - V_0) / S \tag{7}$$

Where $Vcc = 5$ V, $V_o = 1.65$ V (zero-g bias offset), and $S = 0.330$ V/g (nominal sensor sensitivity). Signal processing constraints implemented in MATLAB are outlined in Table 2.

Table 2. Signal processing parameters

Parameter	Setpoint Value	Engineering Description
Baud Rate	119200 bps	Microcontroller-to-PC transmission rate
Sampling Interval (Ts)	0.01 s	Temporal resolution (Fs = 100 Hz)
Buffer Size	1000 points	Total length per experimental window
FFT Window Size	512 points	Discrete Fourier Transform spectral block size

6 Results

6.1 Numerical Modal Extraction

The natural frequencies extracted from the prestressed eigenvalue solutions are presented in Table 3.

Table 3. Finite element natural frequencies (Hz)

Mode	Normal Plate	Lap Joint	Butt Joint	Flanged Joint
1	24.18	23.36	28.79	33.43
2	151.46	152.29	85.24	80.47
3	315.83	278.08	158.90	189.35
4	366.15	364.19	296.71	330.94
5	424.32	397.66	461.11	455.76
6	823.61	941.72	505.71	558.16

6.2 Preload Sensitivity and Frequency Correlation

The numerical modal results show a 5.29% deviation between the monolithic analytical baseline (25.541 Hz) and the finite element plate model (24.188 Hz). This marginal variance is due to the omission of the bolt-hole cutout and the assumption of a uniform cross-section in the analytical beam model.

The analytical and numerical investigations show consistent trends regarding the influence of joint geometry on structural stiffness and modal response. The analytical solution provides an idealized baseline, while the finite element model incorporates geometric discontinuities, contact interactions, and preload effects that more closely represent the physical assemblies.

The introduction of joint geometry alters the fundamental mode frequency. The lap joint exhibits a lower fundamental frequency (23.361 Hz) due to localized interface compliance introduced by the asymmetric plate overlap. Conversely, butt (28.791 Hz) and flanged assemblies (33.435 Hz) shift the fundamental frequency upward. This frequency elevation stems from shorter effective free-cantilever spans, localized mass concentrations around the joint, and localized stiffening from the preloaded fasteners.

6.3 Experimental Dynamic Response

The experimental measurements provide a comparative assessment of the vibration-response characteristics of the investigated joint configurations under identical excitation conditions. While the numerical analysis focuses on modal characteristics and natural frequencies, the experimental investigation evaluates response amplitudes within the accessible operating range of the test system. Together, the numerical and experimental observations offer complementary insight into the influence of joint configuration on structural behaviour.

The peak acceleration responses captured at the free end across variable motor speeds are compiled in Table 4.

Table 4. Peak experimental acceleration responses (m/s²)

Joint Topology	150 RPM (2.0 Hz)	350 RPM (5.0 Hz)	450 RPM (7.5 Hz)
Normal Plate	0.02	0.03	0.06
Lap Joint	0.03	0.03	0.06
Butt Joint	0.03	0.09	0.08
Flanged Joint	0.02	0.03	0.06

7 Discussion

7.1 Interfacial Contact Physics and Preload Mechanisms

The stress fields induced by the 10.3 kN bolt preload generate localized compressive zones across the contact interfaces. At low operational speeds (150 RPM / 2.0 Hz), the dynamic shear forces remain well within the Coulomb friction limits. The mating surfaces remain primarily in a locked state ("stick zone"), preserving high localized contact stiffness.

As the base excitation frequency escalates toward operational limits (350 RPM and 450 RPM), the inertial forces induce a transition from stick to localized microslip. This boundary transition reduces the effective contact area and causes structural softening, manifesting as shifts in the response frequencies and amplitude-dependent damping.

7.2 Geometric Effects on Structural Stability

The experimental and numerical evaluations reveal a clear structural performance trend: Flanged Joint > Normal Plate ≈ Lap Joint > Butt Joint.

Flanged Joint: This configuration retains high geometric stability under elevated base excitations (450 RPM). The symmetric out-of-plane stiffening ribs increase the area moment of inertia, restricting relative slip and maintaining a clean frequency spectrum with low harmonic distortion.

Lap Joint: This assembly exhibits prominent odd-harmonic generation (3× and 5× multiples) under moderate loading. This non-linear distortion is driven by asymmetric load paths and localized rocking modes, causing intermittent stick-slip transitions across the overlapping plane.

Butt Joint: The butt joint demonstrates severe structural instability, with peak accelerations reaching 0.09 m/s² at 350 RPM. Because it relies entirely on localized contact friction across backing plates, the interface undergoes premature macro-slip under high inertial loads. This leads to localized gapping and clapping behavior, scattering the energy across a broad spectrum.

The observed response behavior suggests increased sensitivity to interfacial compliance and localized load-transfer effects.

8 Conclusion

This study characterized the non-linear dynamic behavior of distinct bolted joint configurations using a pre-stressed finite element framework validated by experimental vibration testing. The primary conclusions are:

Preload Stiffening: Bolt preload governs local contact boundary conditions. The pre-stress geometric stiffness matrix shifts the natural frequencies upward, with the flanged joint configuration achieving the highest fundamental frequency of 33.435 Hz.

Dynamic Stability Trends: The structural stability ranking (Flanged > Lap > Butt) was consistent across both numerical and experimental domains. The flanged assembly effectively controls macro-slip, while the butt joint remains highly susceptible to contact breakdown and chaotic frequency distribution under elevated inertial forces.

Non-linear Diagnostics: The emergence of high-order harmonics (2× and 3× multiples) at high RPM levels serves as an experimental indicator of structural softening and full transition into the non-linear stick-slip regime.

Metrology Instrumentation: The close correlation between the experimental data and numerical models demonstrates that cost-effective MEMS data acquisition architectures can reliably identify fundamental structural frequencies in jointed assemblies.

The findings presented in this paper demonstrate the usefulness of combining numerical modelling with experimental vibration assessment for investigating bolted-joint behaviour. The numerical predictions and experimental observations consistently indicate that joint configuration plays a significant role in governing structural response characteristics. The results reported herein are representative of the principal trends observed during the investigation and provide a foundation for more extensive correlation studies in future work.

8.1 Future Scope

Subsequent research will target:

- Developing data-driven models utilizing physics-informed neural networks (PINN) to estimate real-time macro-micro slip boundaries.
- Evaluating multi-bolt arrays under multi-axial random vibration paths.
- Implementing digital twin architectures to track long-term preload attenuation caused by material relaxation and micro-impact embedding.

References

1. W. D. Iwan, "A distributed-element model for hysteresis and its steady-state dynamic response," Journal of Applied Mechanics, vol. 33, no. 4, pp. 893–900, 1966.
2. E. J. Berger, "Friction modeling for dynamic system simulation," ASME Applied Mechanics Reviews, vol. 55, no. 6, pp. 535–577, 2002.
3. Y. K. Wen, "Method for random vibration of hysteretic systems," Journal of Engineering Mechanics Division, vol. 102, no. 2, pp. 249–263, 1976

4. R. Lacayo et al., "Nonlinear modeling of structures with bolted joints: A comparison of two approaches based on a time-domain and frequency-domain solver," Mechanical Systems and Signal Processing, vol. 114, pp. 413–438, 2019.
5. M. Krack et al., "Reducing finite element models of bolted joints using spectral submanifolds," in Proc. Tribomechadynamics Research Challenge, 2022.
6. B. Peeters, H. Van der Auweraer, P. Guillaume, and J. Leuridan, "The PolyMAX frequency-domain method: A new standard for modal parameter estimation," Shock and Vibration, vol. 11, pp. 395–409, 2004.
7. Carrella and D. J. Ewins, "Identifying and quantifying structural nonlinearities in engineering applications from measured frequency response functions," Mechanical Systems and Signal Processing, vol. 25, no. 3, pp. 1011–1026, 2011.
8. M. Varanis, A. L. Silva, P. H. A. Brunetto, and R. F. Gregolin, "Instrumentation for mechanical vibrations analysis in the time and frequency domain using the Arduino platform," RevistaBrasileira de Ensino de Física, vol. 38, no. 1, p. 1301, 2016.
9. C. Reddy, S. Shenoy, and R. S. Sharma, "Vibration analysis of a cantilever beam in time and frequency domain using Arduino platform," VibroengineeringProcedia, vol. 29, pp. 1–5, 2019.
10. Kumar, S.Sendhil, and M. Senthil Kumar, “Condition monitoring of rotating machinery through vibration analysis,” JSIR, vol.73, pp. 258-261, 2014.